

Table of Contents

| | |
|--|-----------|
| 1. INTRODUCTION..... | 7 |
| 1.1 Overview of Mir Photo/TV Survey..... | 5 |
| 1.2 Summary of Findings..... | 6 |
| 1.2.1 Mir Configuration..... | 7 |
| 1.2.2 Mir Survey Coverage and Surface Assessment..... | 8 |
| 1.2.3 Docking Mechanism Assessment..... | 9 |
| 1.2.4 Mir Environmental Effects Payload Analysis..... | 9 |
| 1.2.5 Correlation of Docking Events..... | 9 |
| 1.2.6 Motion Analysis from Video..... | 10 |
| 1.2.7 Debris During Docking Procedure..... | 10 |
| 1.2.8 Imagery Evaluation..... | 10 |
| 1.2.9 Other Analysis..... | 10 |
| 2. MIR CONFIGURATION..... | 11 |
| 3. MIR SURVEY COVERAGE AND SURFACE ASSESSMENT..... | 16 |
| 4. DOCKING MECHANISM ASSESSMENT..... | 28 |
| 4.1 Docking Mechanism Condition..... | 28 |
| 4.2 Target Visibility Comparison..... | 28 |
| 5. MIR ENVIRONMENTAL EFFECTS PAYLOAD ANALYSIS..... | 30 |
| 5.1 Experiment Background..... | 30 |
| 5.2 Surface Assessment..... | 31 |
| 5.3 Panel Orientation..... | 34 |
| 6. CORRELATION OF DOCKING EVENTS..... | 38 |
| 6.1 Motion Analysis at Soft Dock..... | 38 |
| 6.2 Sources of Error..... | 40 |
| 7. MOTION ANALYSIS FROM FILM AND VIDEO..... | 39 |
| 8. DEBRIS SEEN DURING DOCKING OPERATIONS..... | 40 |
| 9. IMAGERY EVALUATION..... | 42 |
| 9.1 Video Review..... | 42 |

Table of Contents

| | |
|---|-----------|
| 9.2 Still Photography Review..... | 42 |
| 10. CONCLUSIONS AND RECOMMENDATIONS..... | 44 |
| 10.1 Summary..... | 44 |
| 10.2 Conclusions..... | 44 |
| 10.3 Recommendations..... | 45 |
| 11. REFERENCES..... | 46 |

APPENDICES

| | |
|--------------------|--|
| Appendix A: | STS-76 Mir Surface Damage / Discoloration |
| Appendix B: | STS-76 Film Scenelist |
| Appendix C: | STS-76 Video Scenelist Information |
| Appendix D: | Sources for Report Imagery |
| Appendix E: | STS-76 Camera Layout |
| Appendix F: | Acronym List |

List of Figures

| | | |
|------------|--|----|
| Figure 1-A | Backaway View of Mir Space Station..... | 9 |
| Figure 1-B | STS-76 Mir Survey Coverage (Top View)..... | 8 |
| Figure 1-C | STS-76 Mir Survey Coverage (Bottom View)..... | 9 |
| Figure 2 | Mir Space Station during Approach..... | 11 |
| Figure 2-A | Kvant..... | 12 |
| Figure 2-B | Mir Base Block..... | 13 |
| Figure 2-C | Kvant-2..... | 14 |
| Figure 2-D | Spektr..... | 15 |
| Figure 3-A | STS-76 Damage Survey (Bottom View)..... | 18 |
| Figure 3-B | STS-76 Damage Survey (Top View)..... | 16 |
| Figure 3-C | Spektr Radiator Comparison..... | 17 |
| Figure 3-D | Base Block Comparison..... | 18 |
| Figure 3-E | Base Block..... | 19 |
| Figure 3-F | Luch Antenna Dish Comparison..... | 20 |
| Figure 3-G | Arm of the Luch Antenna..... | 21 |
| Figure 3-H | Russian Solar Array Carrier Comparison (top)..... | 22 |
| Figure 3-I | Russian Solar Array Carrier Comparison (bottom)..... | 23 |
| Figure 3-J | Cooperative Solar Array Carrier Comparison..... | 24 |
| Figure 3-K | SP#3 Base Block Array..... | 25 |
| Figure 3-L | SP#2 Spektr Solar Array..... | 26 |
| Figure 3-M | SP#2 Spektr Solar Array..... | 27 |
| Figure 4-A | Centerline (Approach)..... | 31 |
| Figure 4-B | Camera A / Centerline (Approach)..... | 29 |
| Figure 4-C | Camera A / Centerline (Backaway)..... | 29 |
| Figure 5-A | Composite View of MEEP Panels on Docking Module..... | 31 |
| Figure 5-B | MEEP Panels as Seen from PLB Cameras B and D..... | 32 |
| Figure 5-C | MEEP Panels as Seen from Camera C..... | 33 |
| Figure 6-A | Centerline Video at First Contact..... | 36 |
| Figure 6-B | Docking Ring Interface at First Contact..... | 37 |
| Figure 6-C | Motion Analysis at Docking as a Function of Time..... | 38 |
| Figure 7-A | Orbiter to Mir Distance Comparison using TCS and Video Data..... | 39 |
| Figure 8-A | Debris Near Payload Bay..... | 40 |
| Figure 8-B | Tumbling Debris from the Docking Module..... | 41 |

List of Tables

Table 5-A Panel Surface Normal Vectors (in Orbiter Coordinates).....35

List of Tables

1. INTRODUCTION

NASA and RSC-E are involved in a cooperative venture in which the Shuttle will rendezvous with the Mir Space Station during several missions over the next two years. This sequence of at least six missions will serve as a precursor to the two nations' involvement in the International Space Station. The rendezvous missions provide NASA scientists and engineers an opportunity to study the orbital, dynamic, and environmental conditions of long duration spacecraft, as well as develop evaluation and risk mitigation techniques which have direct application to the International Space Station.

STS-76 launched on March 22, 1996, and was docked to the Mir Space Station from the 24th through the 29th. The ten day mission ended on March 31, 1996, at Dryden Flight Research Center. This was the Shuttle's third docking mission and its fourth rendezvous with the Mir Space Station. As part of Detailed Test Objective 1118 (DTO-1118), approximately 1300 photographs and 22 hours of video of the Mir Space Station were acquired during the mission. This report documents results from survey-related imagery analysis tasks.

Results of Detailed Test Objective (DTO-1118) imagery analysis from STS-63, STS-71 and STS-74 were documented in earlier reports. The STS-63 JSC/RSC-E Mir Survey Joint Report (JSC # 27246) was released in September 1995, and the STS-71 JSC/RSC-E Mir Survey Joint Report (JSC # 27355) was released in January 1996. These reports include evaluation of the Mir imagery by RSC-Energia. The STS-74 JSC Mir Survey Report (JSC #27383) was released in February 1996. The joint report for STS-74 is currently in review.

1.1 Overview of Mir Photo/TV Survey

DTO-1118 integrates the requirements for photographic and video imagery of the Mir Space Station generated by the engineering and science communities within NASA. Although mission requirements vary, the principal objectives of the Mir Photo/TV Survey are as follows:

- Study the effects of the space environment on a long-duration orbiting platform.
- Assess the overall condition of the Mir.
- Provide assurance of crew and Orbiter safety while in the proximity of the Mir Space Station.
- Understand the impact of plume impingement during proximity operations.
- Evaluate the equipment and procedures used to gather survey data.

The Image Science & Analysis Group (IS&AG) conducted several analysis tasks (based on user requirements) using the returned imagery data from STS-76. They were to:

- Verify the configuration of the Mir complex.
- Assess the effect of micrometeoroid impacts and other visible damage on Mir surfaces.
- Compare the condition of Station surfaces to that seen on past missions.
- Document the condition of the docking mechanism.
- Characterize debris seen during and after docking operations.

Determine the usefulness of image data in calculating approach and backaway velocities.

Survey the Docking Module and the attached Cooperative and Russian Solar Arrays (CSA and RSA).

Determine the pointing angles and initial surface condition of each of the Mir Environmental Effects Payload (MEEP) panels installed on the docking module.

Correlate target motion seen during the docking procedure.

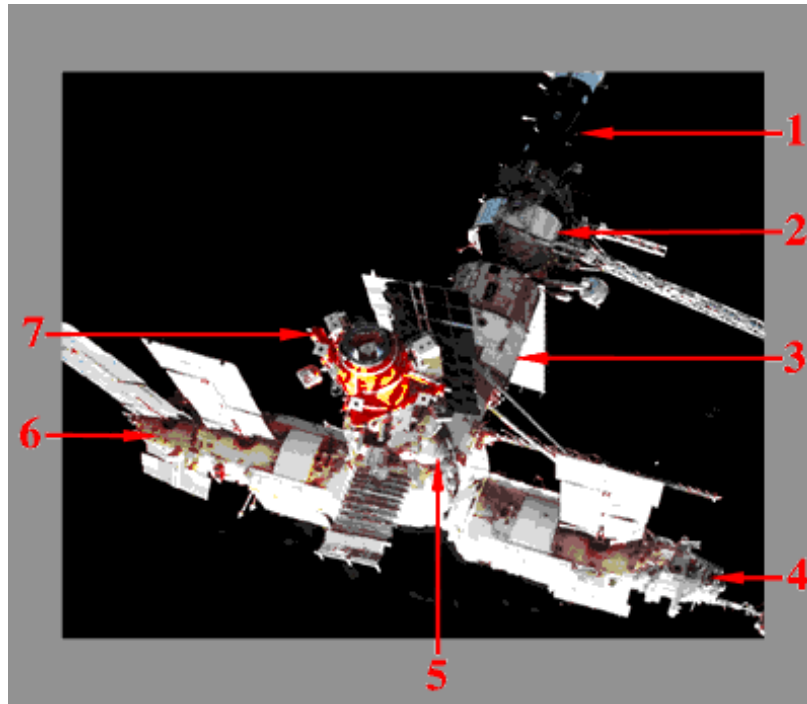
Assess the quality of video and photographic data.

1.2 Summary of Findings

The format of this report differs from those written for earlier rendezvous missions. The Mir Configuration section was used to highlight Station features not previously identified and is not meant to be comprehensive. In the Mir Survey Coverage and Surface Assessment section, images taken during STS-76 are compared to images of the same area from previous missions where applicable. This adds a temporal perspective to the damage and discoloration seen to date. There was no significant solar array motion observed on this mission, so that section has been deleted from this report. In addition, there are two entirely new sections in the report: the Mir Environmental Effects Payload (MEEP) section includes calculations of the orientation of MEEP panels, and the Correlation of Docking Events section contains an analysis of the crosshair alignment target motion at soft dock.

1.2.1 Mir Configuration

Configuration information is important for proximity operations requiring visual navigation and for conducting loads simulations of docked configurations. Available drawings of the Mir Space Station were compared to photography acquired during the rendezvous. The backaway view in Figure 1-A identifies different Mir modules photographed during STS-76.



1. Soyuz
2. Kvant
3. Base Block
4. Kvant-2
5. Kristall
6. Spektr
7. Docking Module

1.2.2 Mir Survey Coverage and Surface Assessment

The purpose of this surface assessment is to study the effects of the space environment on Station materials. This survey included analysis of all visible module and solar array surfaces. The configuration of the Mir Space Station for STS-76 was essentially the same as it was for STS-74. This provided an excellent opportunity to compare changes to the same surface areas over time. One of the most dramatic comparison was between the images taken of the Spektr radiator facing the Orbiter. The views of the radiator surface taken during STS-76 show how areas of paint, beginning to blister on STS-74, are now completely gone. Discoloration of features on the Docking Module, which had only been in space for four months, is quite dramatic. A comparison between Base Block images revealed apparent abrasion to the discoloration seen on the surface. Coverage of the Luch antenna dish from STS-76 was compared to imagery from STS-63. Comparison of the images revealed little change in the discoloration of the antenna dish. However, other views reveal significant discoloration of the antenna arm. Although this discoloration was seen on previously acquired Russian photography, this is the first time imagery of this area has been taken for DTO-1118. Close-up images of the SP#3 Base Block array revealed at least two cells on outer panels of the array which have sustained surface damage. The front sides of the SP#2 and SP#4 arrays on Spektr were photographed for the first time. There were several areas of discoloration on these arrays. Figures 1-B and 1-C document the extent of detailed and overview (i.e., video and/or fly-around still photography) coverage of the Mir Space Station acquired during STS-76.

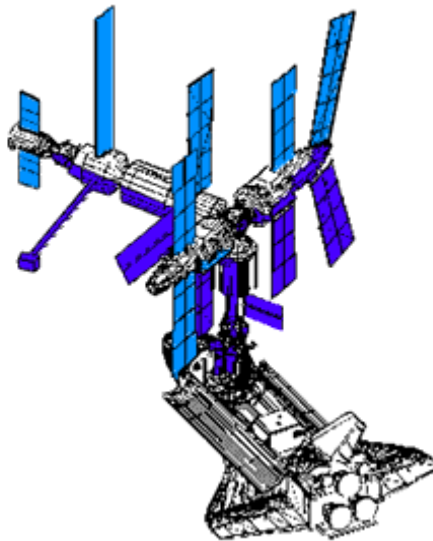


Figure 1-B STS-76 Mir Survey Coverage (Top View)

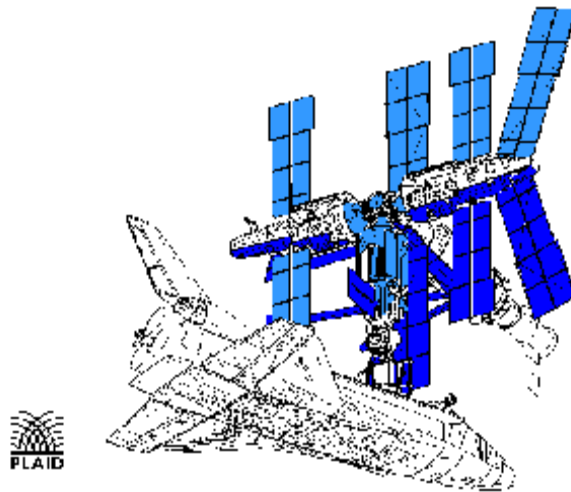


Figure 1-C STS-76 Mir Survey Coverage (Bottom View)

1.2.3 Docking Mechanism Assessment

An overall assessment of the docking mechanism and its visible targets is made on each rendezvous mission. Only video footage was acquired of the docking mechanism and target before and after the rendezvous. In general, video imagery showed the mechanism area and latch assemblies appeared to be free of damage and in good condition during both approach and backaway.

1.2.4 Mir Environmental Effects Payload Analysis

Four Mir Environmental Effects Payload (MEEP) panels were installed on the Docking Module during an EVA on STS-76. A survey of each panel was performed using payload bay cameras to note the initial deployment condition. No visible damage was seen on any of the Orbiter-facing panel surfaces. In addition, verification of each panel's orientation was determined photogrammetrically using both aft payload bay cameras. These orientation angles are presented as surface normal unit vectors in Table 5-A.

1.2.5 Correlation of Docking Events

Analysis was performed on the docking sequence in an attempt to correlate events with times. Problems with timing on the vertical interval of the recorded video limited the analysis to a comparison of relative times between events. Three different events were tracked: the separation between the Orbiter and Mir docking rings through soft dock, the first lateral movement of the washer seen on the centerline camera view, and the first lateral movement of the standoff docking target. Each of these events can be identified on the plot displayed in Figure 6-C.

1.2.6 Motion Analysis from Video

Payload bay camera video data was used to measure the relative motion between the Shuttle and Mir. During approach and backaway procedures, the Trajectory Control System (TCS) was used to determine distances from the Orbiter to the Mir Space Station. This trajectory data was compared to calculations made from photogrammetric analysis of the video. Errors resulting from the video analysis were on the order of +/- 5 percent (under good lighting conditions). This comparison will help future motion analyses when only imagery sources are available.

1.2.7 Debris During Docking Procedure

Several small pieces of debris were seen during the docking sequence. Three of these pieces of debris were tracked and characterized and are considered representative of the particles around the time of docking. The velocity of two of these pieces was estimated to approximately 2 inches per second. The velocity of the third piece was estimated to be 5 inches per second. None of the visible debris was seen making contact with the Mir Space Station.

1.2.8 Imagery Evaluation

STS-74 image data and acquisition procedures were evaluated. Assessment of image data was performed to identify problems with procedures and equipment for subsequent rendezvous missions. In general, good video and photographic coverage of Station surfaces was obtained during the docked phase of the mission. However, limited imagery was acquired during the approach and backaway. This mission marked the third time that the Electronic Still Camera (ESC) was available for image acquisition during the rendezvous missions. However, DTO-1118 coverage provided by the ESC was limited in its detail.

1.2.9 Other Analysis

Individual video frames were digitized and enhanced to verify the angle of the Base Block SP#2 array in response to a request from Structures and Dynamics engineers. This enhanced imagery showed that the array was not in the planned feathered position. This position was designed to optimize clearance and minimize plume impingement effects.

Besides minor vibrations noted at the tip of Base Block SP#2 during video surveys, no array motion was documented on this mission. The minimal amount of solar array motion detected could be attributed to limited coverage of modules and arrays during approach and backaway.

2. MIR CONFIGURATION

A detailed assessment of the STS-76 configuration is presented. This involved identifying and labeling features directly from the photography. A comparison of expected and actual Station elements revealed features that were not identified in the documentation. These features are labeled as ‘unknown’ in the following images and will be discussed with Russian investigators. Features not previously identified, as well as changes to the known configuration, are also identified on the following images.

Figure 2 shows the Mir Space Station as it appeared during the STS-76 approach.

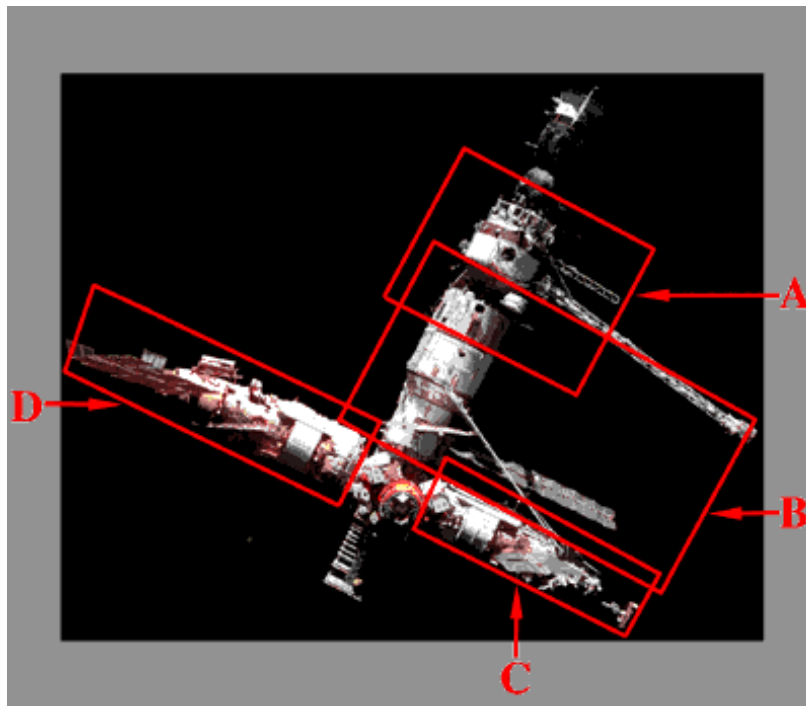


Figure 2 Mir Space Station during Approach

The boxes labeled A-D encompass regions whose exteriors are described in detail within this section. Kvant (A) is an astrophysics and attitude control module. The Base Block (B) is the core module of the Station and provides habitation, power, thermal control and life support. Kvant-2 (C) supports extravehicular and remote sensing activities. The Spekt module (D) is used to study the Earth’s environment and atmosphere.

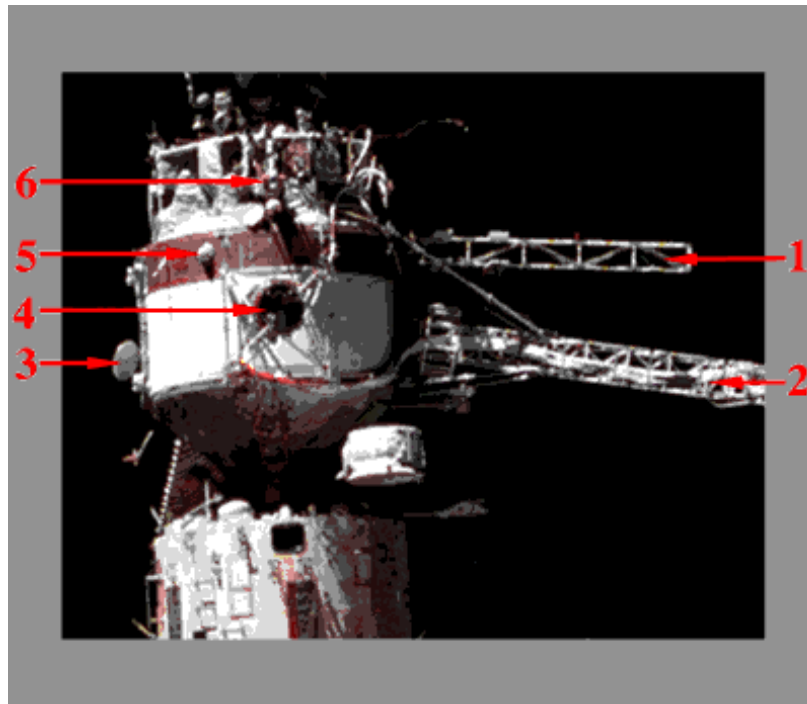


Figure 2-A Kvant

- 1. Rapana Truss***
- 2. Sofora Truss**
- 3. Window Cover**
- 4. Solar Array Attach Point**
- 5. Infrared Sensor**
- 6. Astrosensor**

*First identification of feature.

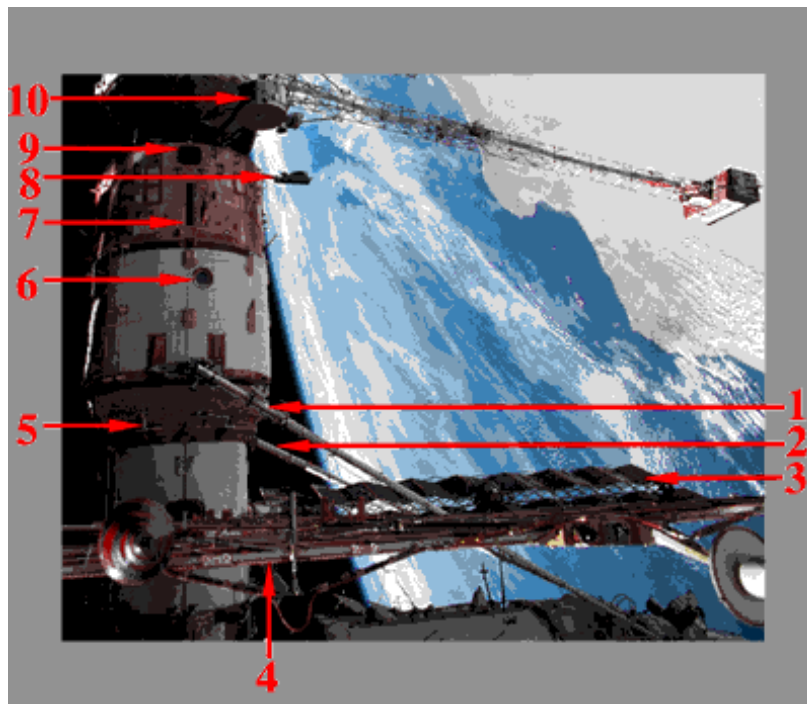


Figure 2-B Mir Base Block

- 1. New "Strehla" EVA Transfer Aid***
- 2. "Strehla" EVA Transfer Aid**
- 3. Base Block Array #3**
- 4. Base Block Array #2**
- 5. EVA Handrails**
- 6. Window**
- 7. Micrometeoroid Impact Sensor**
- 8. Approach & Rendezvous Antenna**
- 9. Attitude Control Thrusters**
- 10. Luch Antenna**

*New feature identified for this mission.

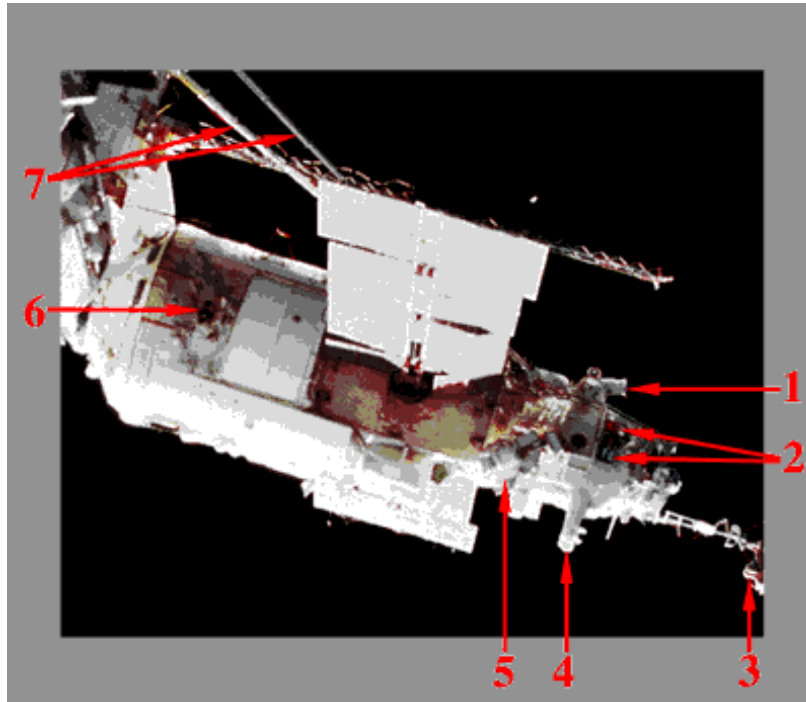


Figure 2-C Kvant-2

- 1. Star Orientation Sensor**
- 2. Materials Experiment**
- 3. Manned Maneuvering Unit***
- 4. Infrared Orientation Device**
- 5. Television Camera**
- 6. Attitude Control Engines**
- 7. “Strehla” EVA Transfer Aids**

*New feature identified for this mission.

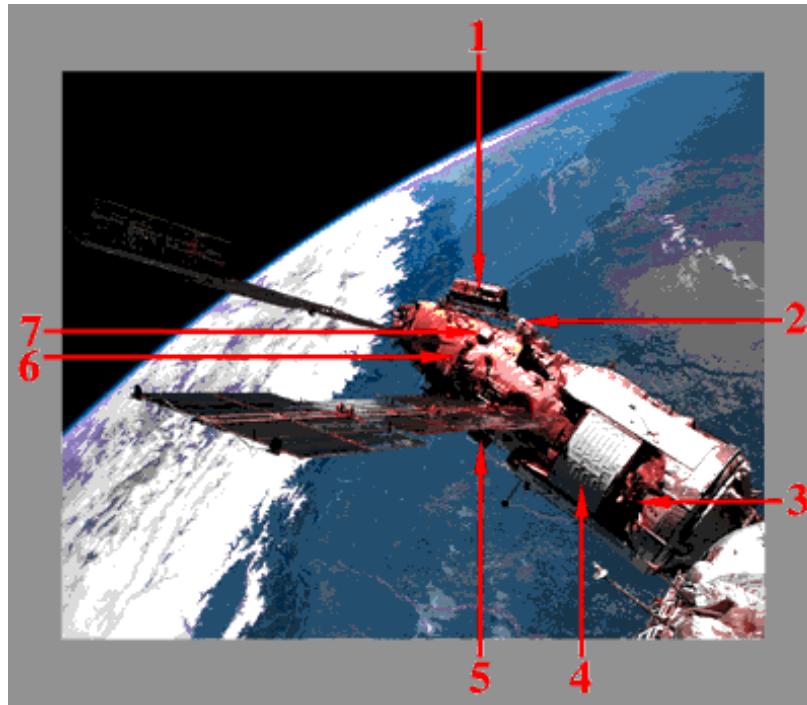


Figure 2-D Spektr

- 1. Belgian Mass Spectrometer (MIRAS)***
- 2. *Unknown***
- 3. Precision Attitude Control Thrusters**
- 4. Radiator**
- 5. Payload Pointing System**
- 6. Attitude Control & Docking Thrusters**
- 7. *Unknown***

*First identification of feature.

3. MIR SURVEY COVERAGE AND SURFACE ASSESSMENT

A survey of the visible Mir Space Station components was performed to identify areas of damage and discoloration. Regions of interest photographed during STS-76 are compared to images of the same area taken during previous missions. Appendix A lists the visible damage and discoloration found in this survey imagery. In addition, the list serves as a cross-reference for damaged areas seen during STS-63, STS-71, and STS-74. Figures 3-A and 3-B show the extent of damage seen on STS-76.

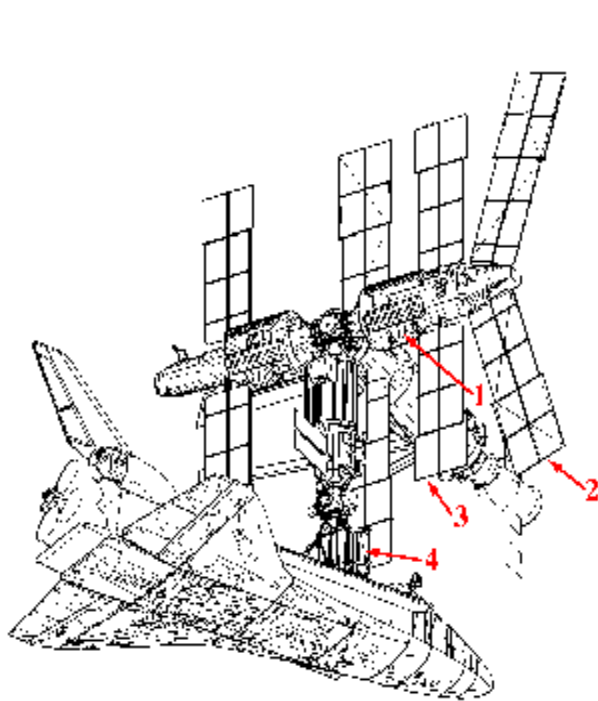


**Figure 3-A STS-76 Damage Survey
(Bottom View)**

1. Spektr radiator with chipped paint.
2. SP#4 Spektr array with surface damage.
3. SP#2 Spektr array with surface damage.
4. Russian Solar Array (RSA) Carrier with discoloration and chipped paint.

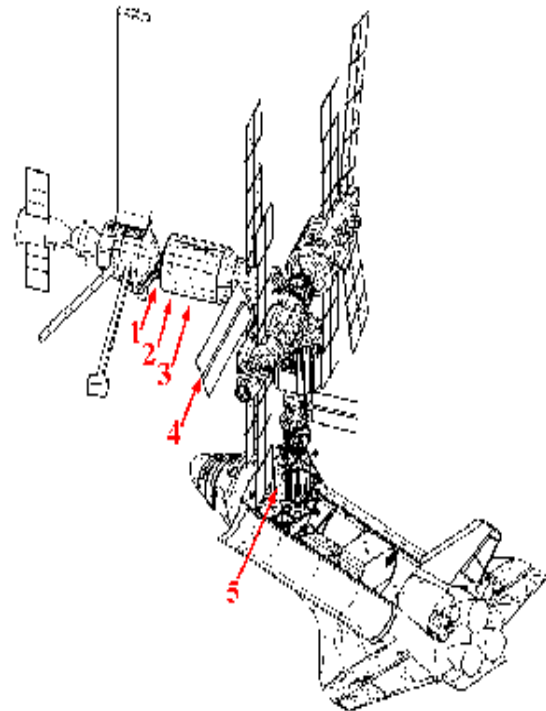


**Figure 3-B STS-76 Damage
Survey (Top View)**

1. Luch antenna discoloration.
2. Base Block surfaces with discolored and chipped paint.
3. Base Block surfaces with chipped paint and micrometeoroid sensor damage.
4. SP#3 Base Block array with surface damage to cells on outer panels.
5. Cooperative Solar Array (CSA) Carrier with discoloration and chipped paint.

The side of Spektr visible during the docked phase of STS-76 is identical to that seen on STS-74. This provides an opportunity to compare the surface on this side of Spektr across the two missions. Figure 3-C shows the radiator adjacent to the Spektr SP#2 array.

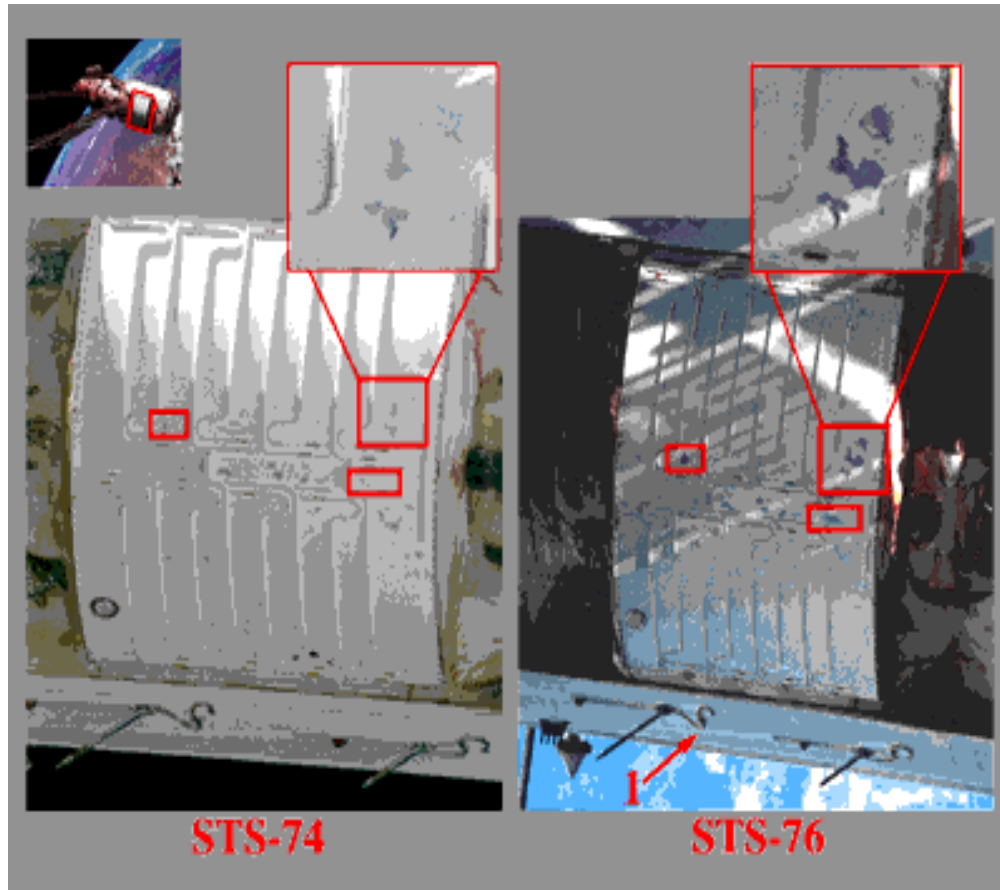


Figure 3-C Spektr Radiator Comparison

Over 50 areas of chipped paint on the surface of the radiator were identified. Correcting for the curvature of the radiator, the area of chipped paint was approximately 800 cm² during STS-74. This area increased in size to approximately 1300 cm² in the four months between STS-74 and STS-76.

The digitized image was thresholded to distinguish clean surfaces from areas with chipped paint. The total area of surface blemishes on the radiator was then generated by summing the number of pixels and scaling this value to represent the actual surface area.

Annotation 1 in the STS-76 image points to one of the white streaks visible on the outer radiator. Apparently, the antennas protruding from the radiator block a source of contamination which is discoloring most of the radiator surface.

The boxes indicate regions of direct correlation between the two missions. In these boxes, the increased area of chipped paint is most readily seen.

Figure 3-D is a comparison of Base Block images between STS-74 and STS-76. Most of the surface discoloration appears unchanged between these two missions.

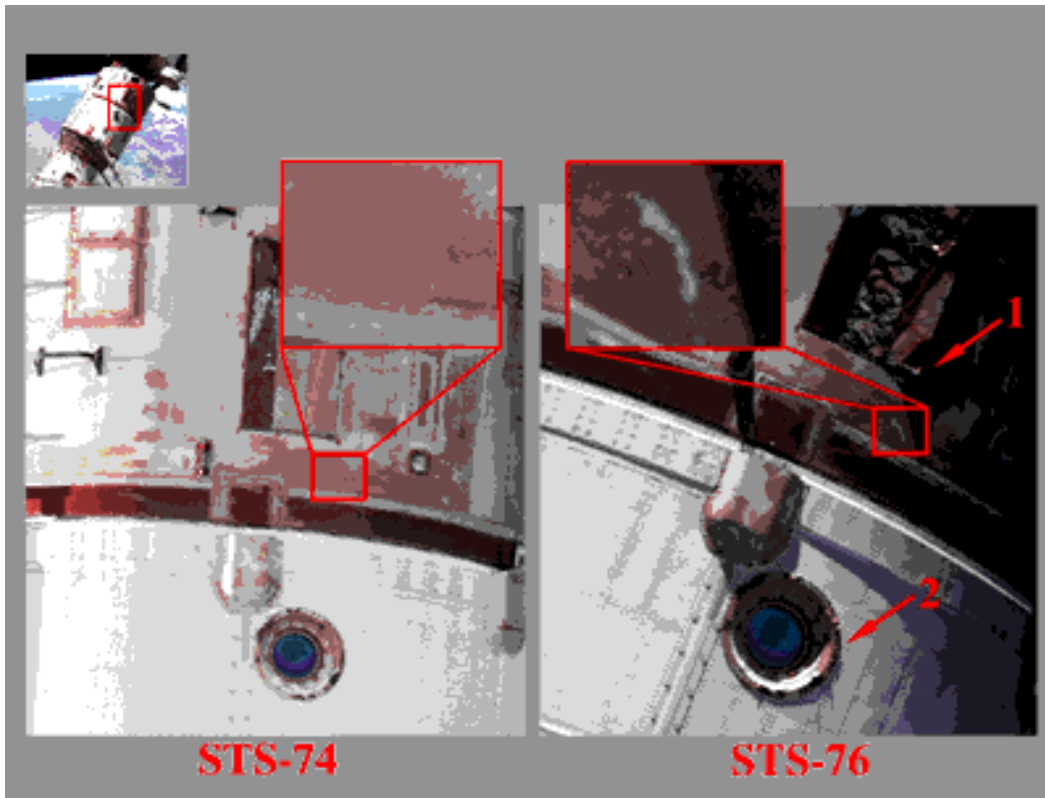


Figure 3-D Base Block Comparison

The highlighted region shows a white area visible on STS-76 which was not present during STS-74. Surface discoloration appears to have been scratched off between these two missions, revealing a white surface below. This scratching may have occurred during a cosmonaut EVA. Discoloration adjacent to this white area appears highly textured. This suggests that the discolored surface material is somehow lifting away from the module.

Item 1 points to the corner of the micrometeoroid sensor which appears to be detached based on the shadows it casts on the module surface. The oblique lighting makes the area lifting up look more dramatic than previous images of the same area and the amount of damage appears to be the same across the two missions. A comparison of imagery taken from the past two missions indicate that the strip was lifted off the surface on STS-74. This strip was measured to be approximately 95 cm by 15 cm in the STS-63 report. The sensor is composed of three of these strips.

Item 2 points to a port window with several areas of chipped paint around its outer edge. The amount of chipping does not appear to have changed between STS-74 and STS-76.

Figure 3-E is an image of the Base Block surface adjacent to the Kvant interface.

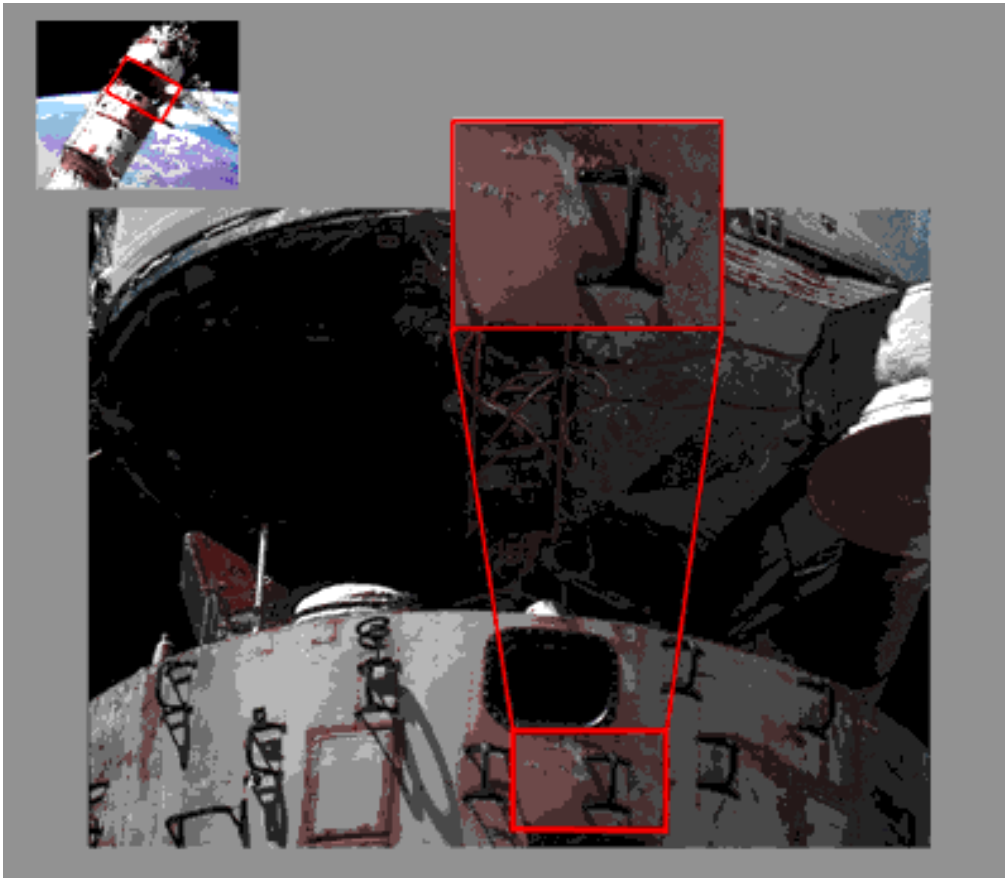


Figure 3-E Base Block

The enlarged area illustrates how discoloration on some areas of the Base Block is blistering and chipping off, revealing the smooth white surface below. The texture of the chipping paint is highlighted by lighting from an oblique angle. The chipping of the discolored area may have been caused by cosmonauts during an EVA. This is especially likely since the region highlighted in this image is surrounded by the hand holds that cosmonauts use for movement around the surface of Mir. The area of blistering and chipping paint appears the same as it did on STS-74.

Figure 3-F is a comparison of Luch antenna images taken during STS-63 and STS-76. The antenna is located on the end of the Base Block at the interface with Kvant.

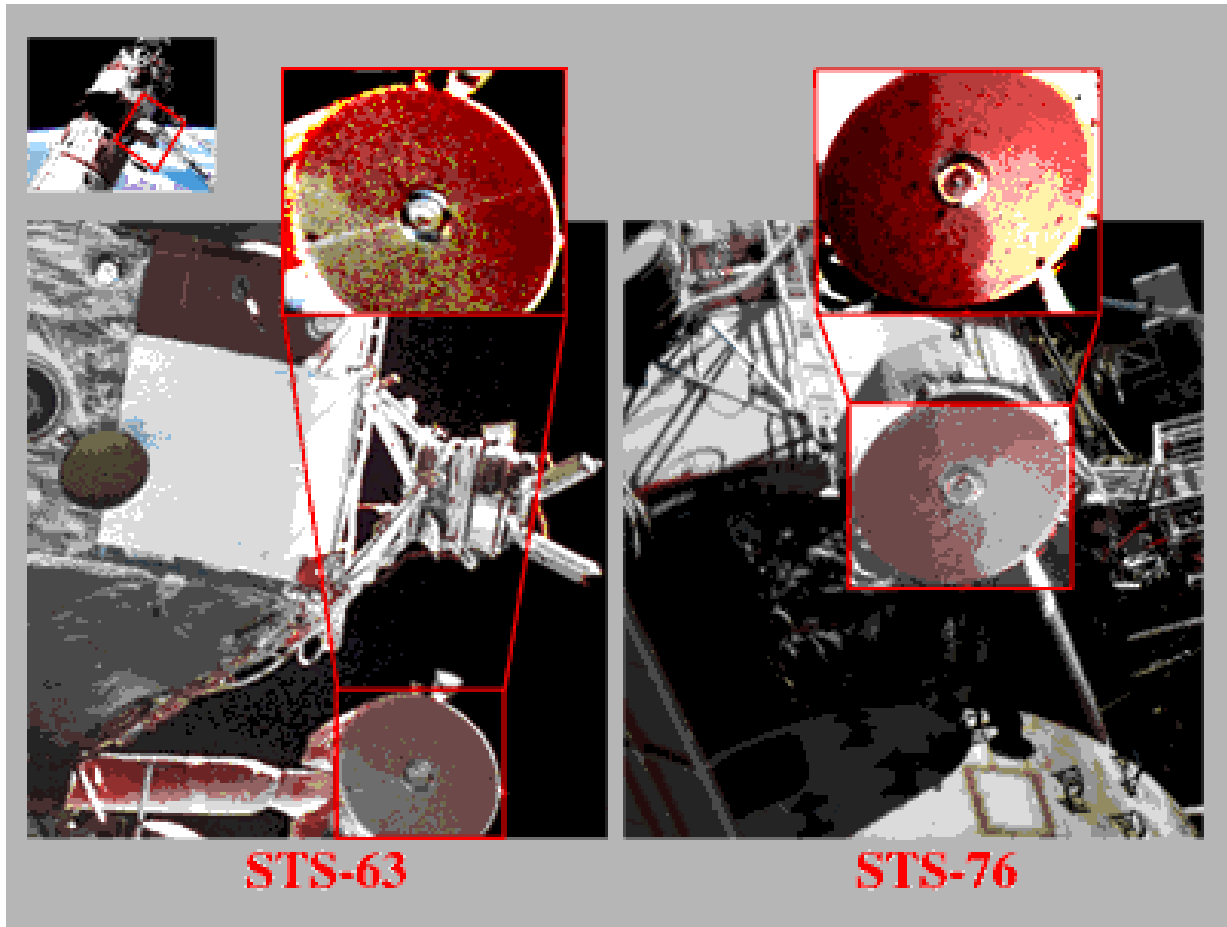


Figure 3-F Luch Antenna Dish Comparison

Figure 3-F shows the front face of the Luch antenna dish. Although the difference between discoloration patterns appears significant, much of this is due to the sharpness difference between the two images. Other factors such as lighting and the resolving power differences between the Nikon (STS-63) and Hasselblad (STS-76) must also be considered when comparing these frames. A detailed examination indicated that the pattern of discoloration on the dish was actually very similar across both missions. This would indicate that the phenomena which caused most of the visible discoloration occurred prior to STS-63 and that no significant changes have occurred since.

Figure 3-G represents the most detailed image of the Luch antenna arm obtained to date. The Luch antenna is located on the end of the Base Block at the interface with Kvant.

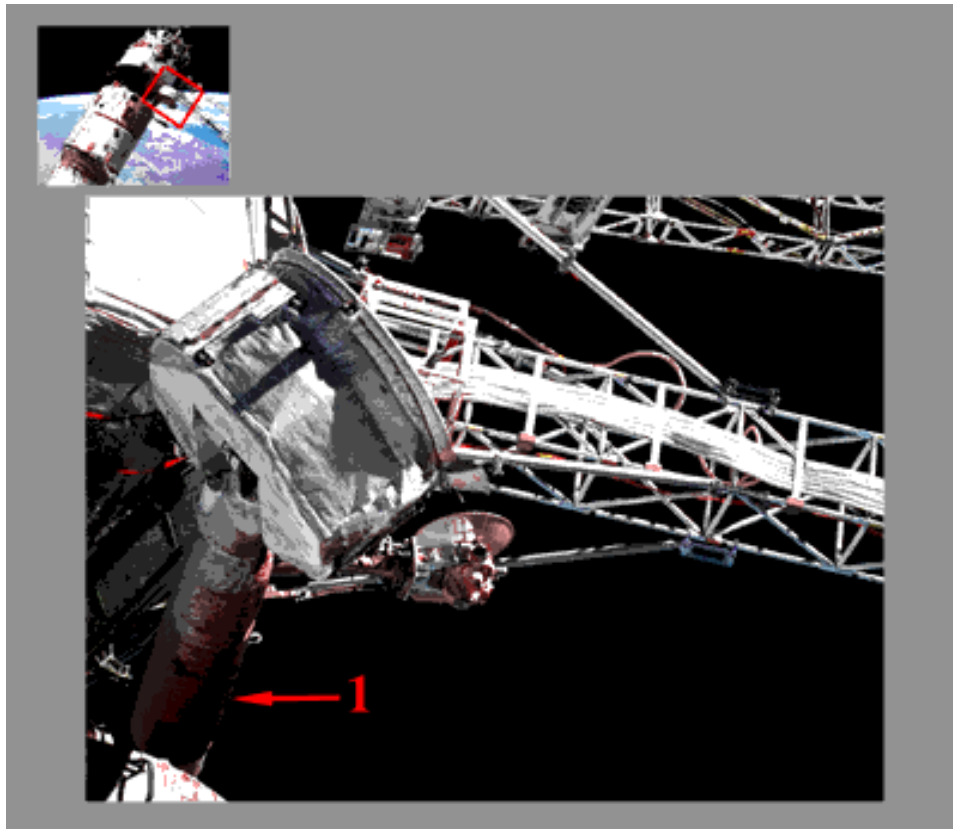


Figure 3-G Arm of the Luch Antenna

The contamination on the arm of the Luch antenna (Item 1) appears to be caused by the same source as that discoloring the end cone of Kvant since the color and pattern of discoloration appears the same as that on the end cone. Materials specialists believe this may be related to fuel line purges. Thermal control system leaks may also contribute to the problem.

Figure 3-H is a comparison of video coverage of a region on the Russian Solar Array (RSA) mounted on the Docking Module. The Docking Module was attached to the Mir complex on STS-74 in November 1995.

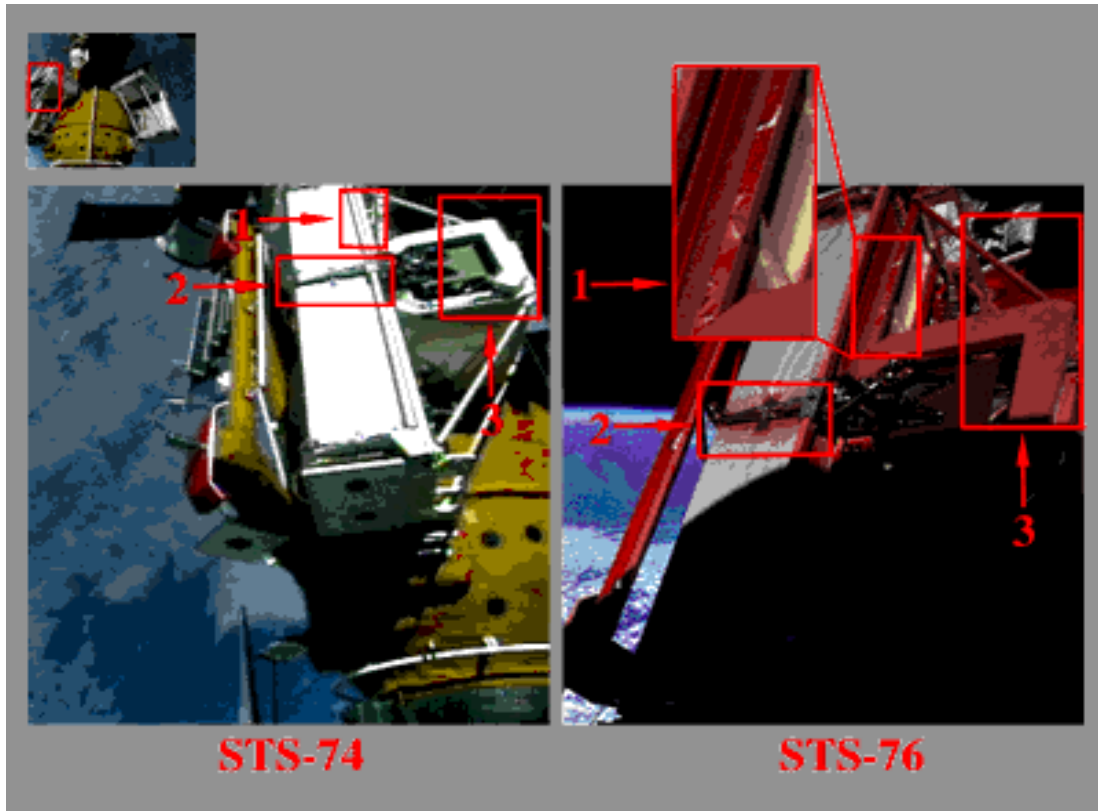


Figure 3-H Russian Solar Array Carrier Comparison (top)

STS-76 imagery shows paint blistering and chipping on two areas of the RSA.

Item 1 in the figure above illustrates where paint is chipping along the RSA carrier.

Item 2 in the figure above highlights brown discoloration around a latch mechanism.

Item 3 in the figure above highlights the general brown discoloration seen along the outer edges of the carrier which were originally white when the RSA was deployed during STS-74.

Note that the general pattern of discoloration has occurred during the 4 months between STS-74 and STS-76. This is especially of interest to investigators since the Mir Environmental Effects Payload (MEEP) panels were attached to the Docking Module on STS-76. The source for the contamination seen on the Docking Module may affect panel surfaces in the future.

Figure 3-I is a comparison of views of the bottom of the Russian Solar Array (RSA) mounted on the starboard side of the Docking Module.

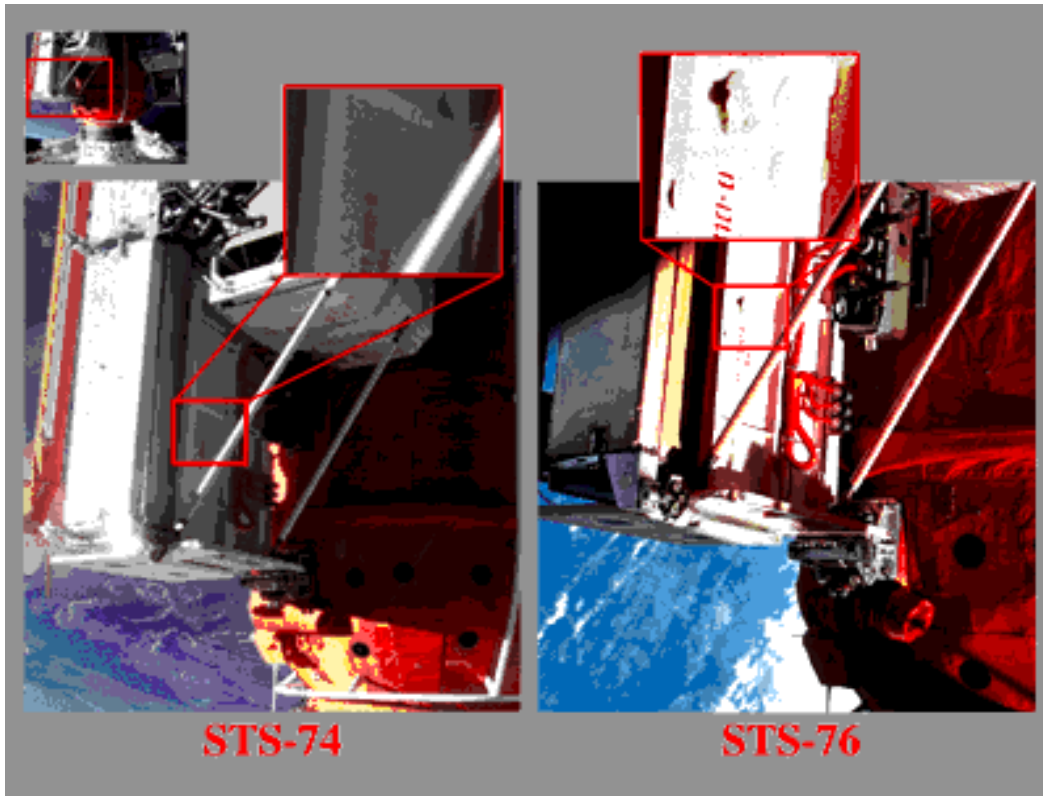


Figure 3-I Russian Solar Array Carrier Comparison (bottom)

The figure above illustrates where paint is chipping along the RSA carrier. In addition, areas along the solar array panels and support arms, which are discolored in the image taken during STS-76, appear white after the Docking Module was installed on STS-74. Note that although shadows affect the color composition of surface features on these images, the uniformity of color along edges seen on STS-74 is in direct contrast to the variation on STS-76. This would indicate the pattern of discoloration is real and not simply variations caused by change in lighting conditions.

Figure 3-J shows comparison views of the Cooperative Solar Array (CSA) mounted on the port side of the Docking Module. The Cooperative Solar Array was deployed on the -Z_B side of the Kvant module during a Russian EVA on May 25, 1996.

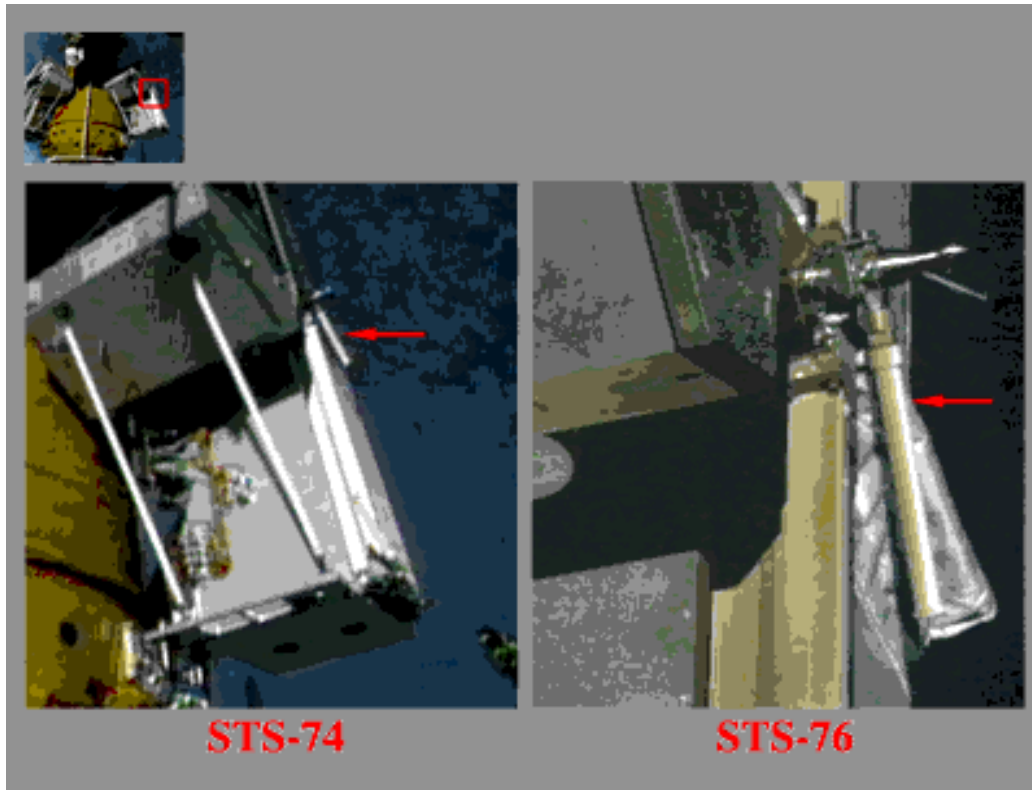


Figure 3-J Cooperative Solar Array Carrier Comparison

Figure 3-J shows areas of discoloration on the CSA structure visible during STS-76. One example of this is the feature attached to the carrier (identified by arrows) in the figure above. The entire pipe appears white on STS-74 video imagery. However, after only four months, one side of the pipe has a brown discoloration, while the other appears to retain its original white color.

A camera bracket used to support a non-axial camera mounted on the Docking Module was retrieved during an EVA on STS-76. In the four months since STS-74, the bracket surfaces facing Russian hardware turned brown while inward surfaces remained their original white color. Investigators who analyzed this bracket in a post-mission study have determined that the surface deposition is composed of silicone. This could be the same contaminant seen on other surfaces of the Docking Module. The preferential pattern of discoloration observed on these structures is significant to the Space Station Vehicle Analysis & Integration Team investigators.

Figure 3-K is an image of the SP#3 array on the Base Block. Images acquired during this mission offer the best views of this solar array to date.

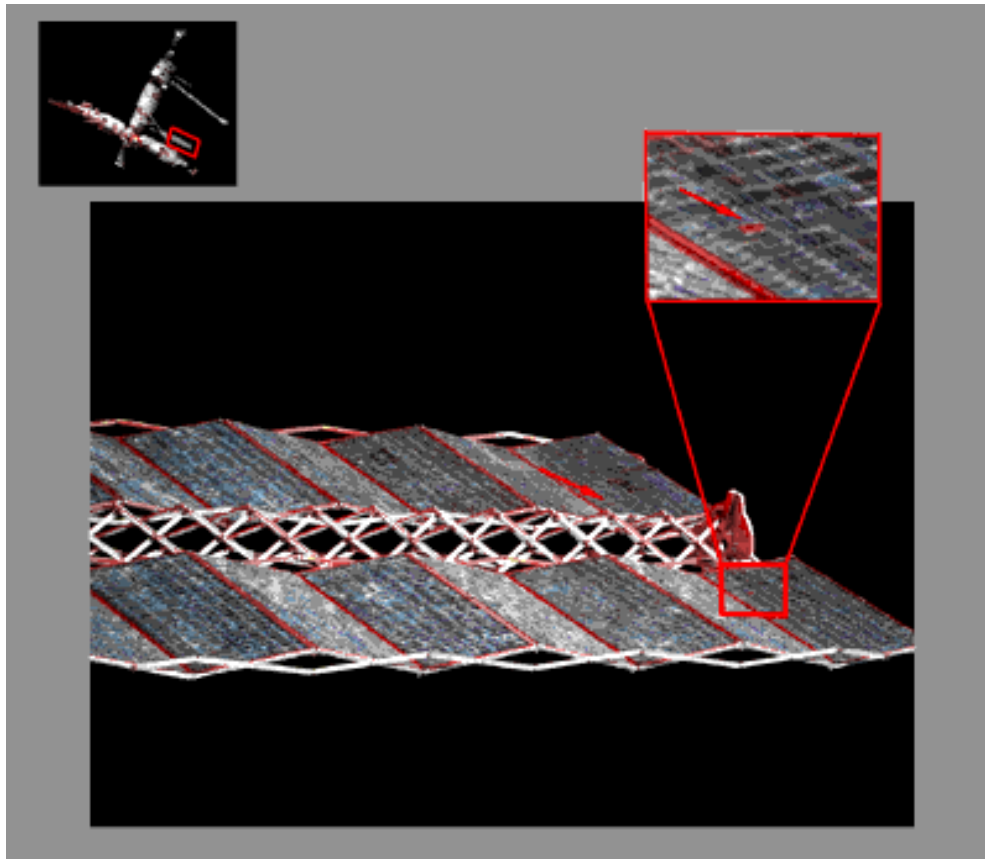


Figure 3-K SP#3 Base Block Array

The arrow in the enlarged image points to a damaged cell on the outer panel of the array. The damage appears to be limited to the cell's top layer and may indicate delamination. A cell on an adjacent panel showing similar damage is identified on the overview image. Each cell measures approximately 4 cm² in area.

Figure 3-L is an image of the front surface of the Spektr SP#2 array. STS-76 provided the first coverage of the front sides of Spektr arrays SP#2 and SP#4.

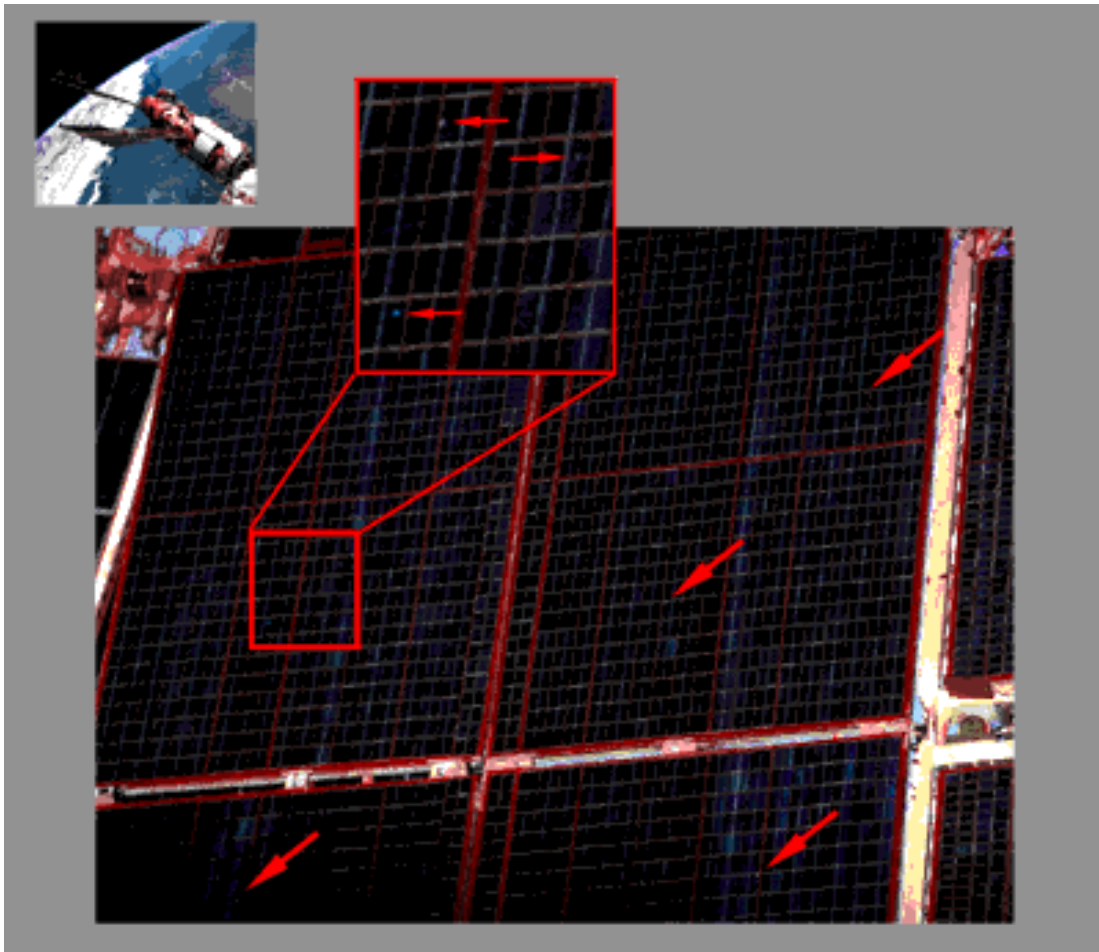


Figure 3-L SP#2 Spektr Solar Array

The arrows in the enlarged region and the arrows on the solar array itself indicate small regions of discoloration. These points, which are lighter in color than the solar cells, may identify possible debris strikes. There are 10 points of discoloration on the array, ranging in diameter from approximately 0.4 to 0.7 cm.

Figure 3-M is an image of the front surface of the Spektr SP#2 array.

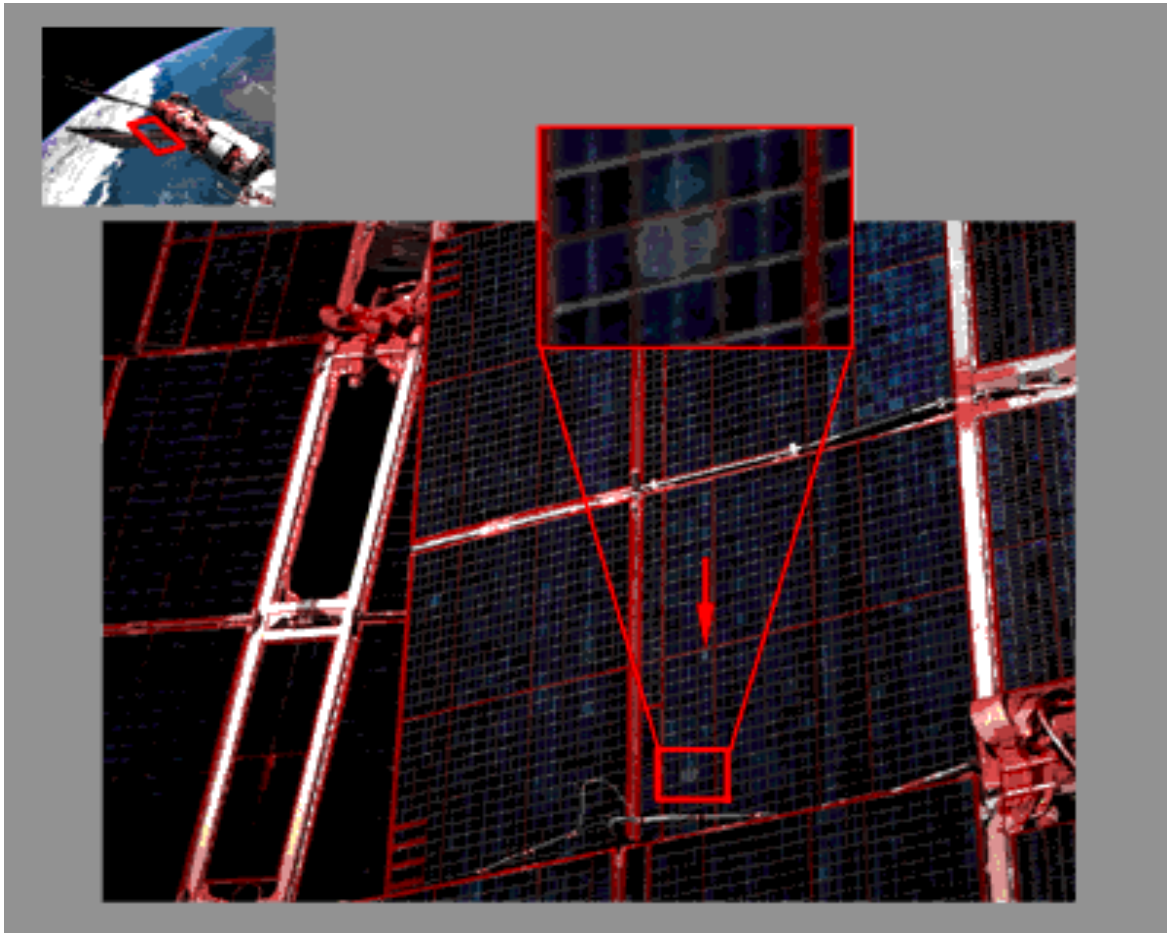


Figure 3-M SP#2 Spektr Solar Array

The enlarged region and the arrow on the solar array indicate areas where the solar array is lighter in color. The discoloration of the two cells in the enlarged region cover an area of approximately 8 cm². The area of discoloration pointed out by the arrow measures approximately 3 cm². There are at least 8 cells exhibiting this type of discoloration and the condition only appears to affect the surface of the cells.

4. DOCKING MECHANISM ASSESSMENT

A survey of the docking mechanism was performed to verify its condition in preparation for STS-79. In addition, a target viewing assessment was conducted to evaluate the performance of the primary video camera (ODS centerline) used during the approach. This view was referenced to those seen on other available cameras. Analysis of these views help in the determination of camera usage for ISS proximity operations.

Through much of the approach phase, the Mir Space Station was in darkness and the CTVC cameras did not reveal any surface detail.

4.1 Docking Mechanism Condition

Due to crew time restraints during final approach, no Hasselblad (70 mm) or Electronic Still Camera (ESC) photographs of the APDU were acquired. Based on the limited video views available, the structural latches, capture latches, body-mounted latches, alignment guides, laser retroreflectors, fluid/electrical socket/plug, and the centerline target all appeared to be in good condition on backaway.

4.2 Target Visibility Comparison

Figures 4-A, B, and C compare views of the docking area taken with two different video cameras. Images of the mechanism and surrounding area were acquired using the ODS centerline video camera during approach and a split screen view using camera A and the ODS centerline video camera during approach and backaway. This comparison is intended to summarize views of the docking mechanism area obtained by the crew.

Since the primary function of the ODS centerline camera was to provide the crew with a means to visually align the target during approach, zoom settings were manipulated at their discretion. Note the zoomed in field-of-view setting of the centerline camera on approach as compared to the backaway. Also, as is the case with all multiplexed views involving the CTVC cameras, the downlinked frames seen on Figures 4-B and 4-C show a color imbalance which is normally corrected in post-processing of the video.

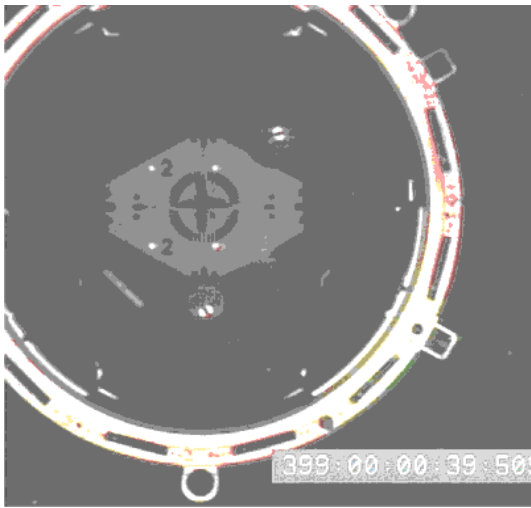


Figure 4-A Centerline (Approach)

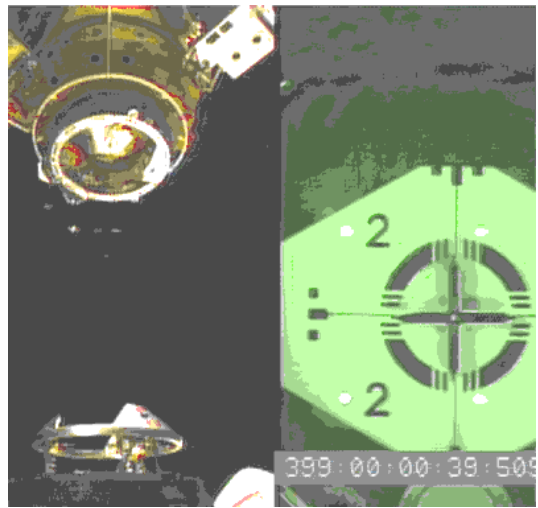


Figure 4-B Camera A / Centerline (Approach)

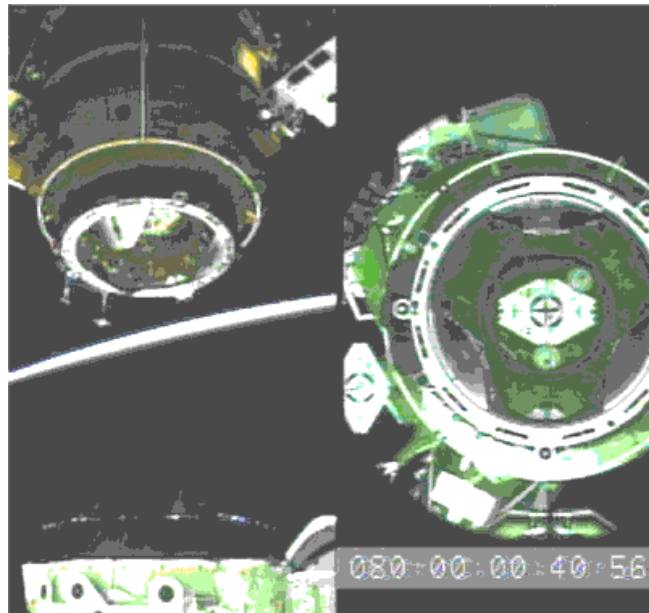


Figure 4-C Camera A / Centerline (Backaway)

5. MIR ENVIRONMENTAL EFFECTS PAYLOAD ANALYSIS

5.1 Experiment Background

The Mir Environmental Effects Payload (MEEP) experiment was attached to the Mir Docking Module during an STS-76 EVA. The MEEP experiment will study the frequency and effects of space debris striking the Mir space station. The MEEP panels also expose selected and proposed International Space Station materials to the effects of space and orbital debris. Because the International Space Station will be placed in approximately the same orbit as Mir, flying MEEP aboard Mir will give researchers an opportunity to test materials for the International Space Station in a comparable orbital environment.

MEEP consists of four separate experiments. The Polished Plate Micrometeoroid and Debris (PPMD) experiment is designed to study debris size, frequency, source and potential damage the debris would cause if it were to hit the station. The Orbital Debris Collector (ODC) experiment is designed to capture orbital debris and return them to Earth to determine the composition of the debris and their possible origins. The Passive Optical Sample Assembly (POSA 1 and 2) experiments consist of various materials that are intended for use on the International Space Station. These materials include paint samples, glass coatings, multi-layer insulation, and a variety of metallic samples.

MEEP is scheduled to remain attached to Mir until late 1997, when the four experiment containers will be retrieved by another space shuttle crew (STS-86) and returned to Earth for study. The data will be studied to determine the type of debris that hits the space station. This information will be useful in understanding how contaminants collect and affect the long-term performance of different surfaces.

Still photography of the MEEP panels was limited to fourteen photographs acquired during the EVA. Of these, most were edge-on views that revealed little about the panel surface conditions. Therefore, all the imagery shown in this section was compiled from a single daylight pass digitized payload bay camera video frames. These views were acquired for two reasons: to verify the initial surface condition of all visible panels, and to determine their orientation. Figure 5-A is a mosaic made up of digitized video frames acquired from payload bay camera B. This type of image provides a higher resolution image (at the expense of color and shadow variations that occur during a daylight pass) than the wide-angle views.

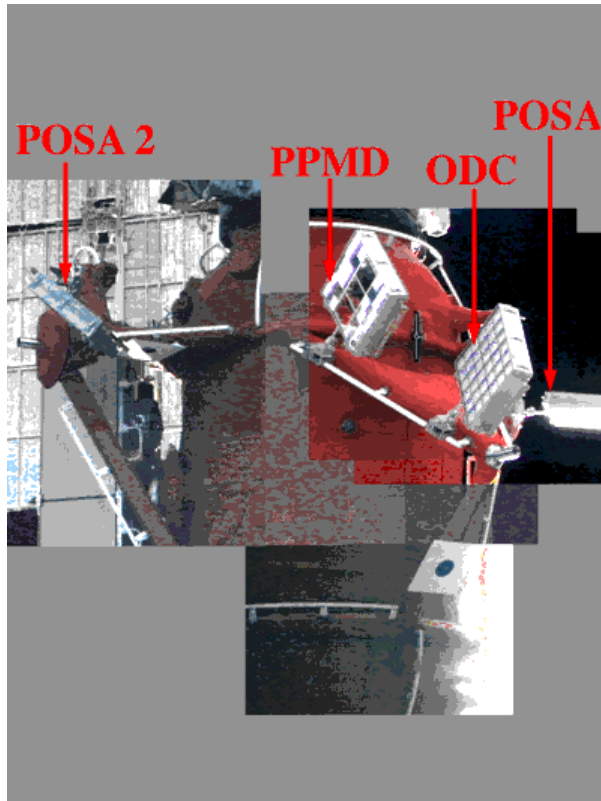
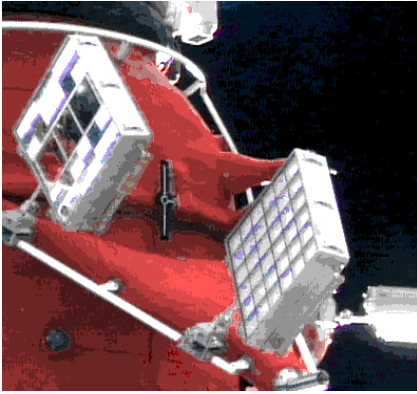


Figure 5-A Composite View of MEEP Panels on Docking Module

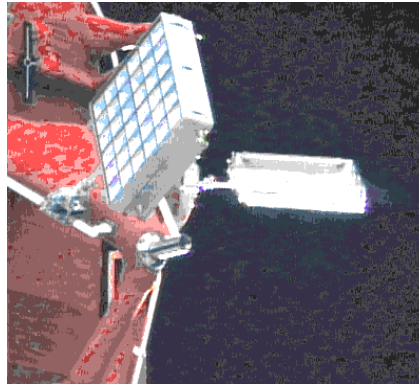
The above image is a composite of 8 video frames taken of the Docking Module from camera B (located on the port aft corner of the payload bay).

5.2 Surface Assessment

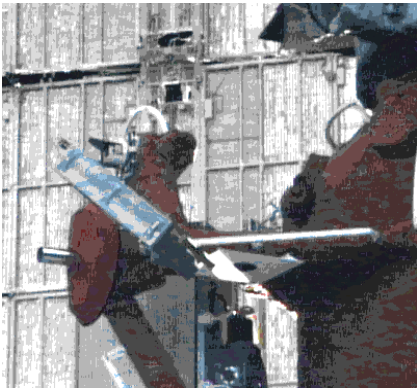
A summary of the available video views is shown in Figure 5-B and 5-C. Note that only the POSA surface could be seen unobstructed from any of the payload bay cameras. This view (from camera D) verified that no visible surface damage occurred to the POSA during installation. All other panels were seen edge-on from the aft cameras. These views do not allow analysis of surface assessment of the other panels. However, none of the panel sides shown in the accompanying digitized video images exhibit surface damage. Similar surveys performed on subsequent missions will try to determine the extent of surface discoloration and damage as a function of time.



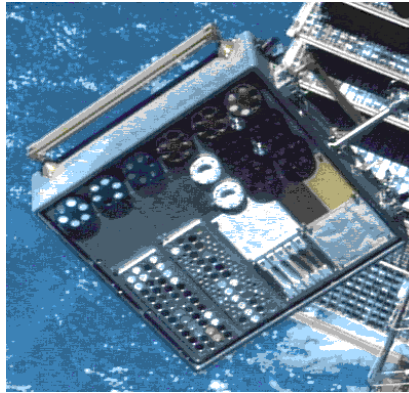
PPMD / ODC



ODC / POSA



POSA 2



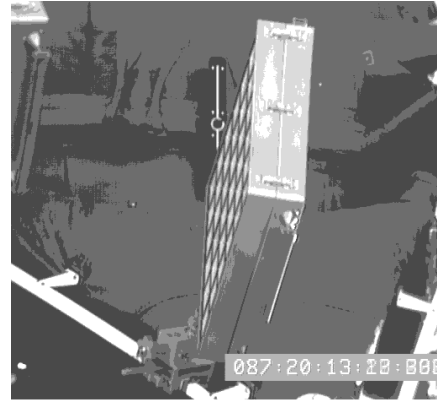
POSA

Figure 5-B MEEP Panels as Seen from PLB Cameras B and D

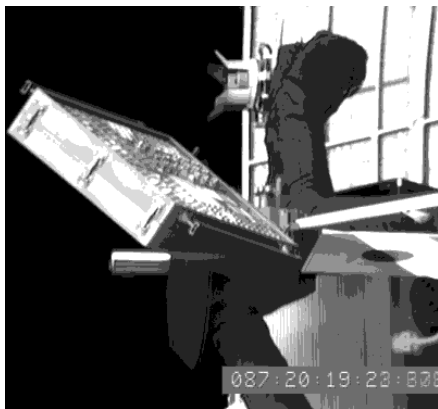
The images above show the best views of each panel from the available CTVC cameras. All but the bottom right image was acquired from camera B located in the aft port corner of the payload bay. The remaining view was obtained from camera D, located in the forward starboard corner of the payload bay. Each of the camera B views was acquired at full zoom, while the camera D view was set to maximize panel features within the field-of-view. Only the Orbiter-facing sides of the PPMD, ODC and POSA panels were seen on these views. No damage was detected on the visible edges or flat surfaces based on these views.



PPM-D



ODC



POSA 2



POSA

Figure 5-C MEEP Panels as Seen from Camera C

The images above show the best available views of MEEP panels as seen from the MLA camera located in the aft starboard corner of the payload bay. Note that although tighter views of each panel were obtained with this camera, much of the detail seen on the CTVC camera is lost. However, these views were useful for determination of the MEEP panel pointing angles.

5.3 Panel Orientation

MEEP investigators requested verification of panel pointing angles to better understand the potential effect of Station thruster plume or outgassing sources on the experiment. These angles were determined analytically using video data obtained from both aft payload bay cameras. The analysis procedure was as follows:

- (a) The pointing angle of each panel with respect to the camera was determined. Setting the camera field-of-view as a variable, a least squares, iterative solution for the panel pointing angle was then generated. Known panel dimensions and actual image coordinates were incorporated into the procedure.
- (b) The panel pointing angle was then rotated into the Orbiter reference system. An initial estimate of each panel's location was provided by the MEEP principal investigators and was used in the calculation of camera pan and tilt angles, since the lack of background points within the scene precluded the direct determination of the camera pointing. The use of pre-mission panel location estimates is not believed to be a significant source of error.
- (c) The surface normal unit vector was then calculated with respect to Orbiter coordinates. Direction cosines generated by the camera pan and tilt angles were used in the calculation of these final pointing angles. Both cameras B and C were used to arrive at independent solutions for the normalized vector. Since the accuracy of each camera's solution was not quantifiable, the results were averaged and a new unit vector generated.

| | | Xo | Yo | Zo |
|----------------------|---|---------------|---------------|---------------|
| <u>ODC</u> | Predicted | -0.332 | 0.943 | 0.004 |
| | Calculated average of (2) camera solutions | -0.348 | 0.934 | -0.079 |
| | (+/-) precision between the (2) camera solutions | 0.167 | 0.048 | 0.167 |
| <u>POSA</u> | Predicted | 0.000 | 0.000 | -1.000 |
| | Calculated average of (2) camera solutions | -0.043 | 0.064 | -0.997 |
| | (+/-) precision between the (2) camera solutions | 0.004 | 0.156 | 0.010 |
| <u>POSA 2</u> | Predicted | -0.170 | -0.686 | -0.707 |
| | Calculated average of (2) camera solutions | -0.295 | -0.703 | -0.647 |
| | (+/-) precision between the (2) camera solutions | 0.090 | 0.047 | 0.092 |
| <u>PPMD</u> | Predicted | -0.332 | 0.943 | 0.004 |
| | Calculated average of (2) camera solutions | -0.351 | 0.936 | 0.005 |
| | (+/-) precision between the (2) camera solutions | 0.167 | 0.063 | 0.000 |

Table 5-A Panel Surface Normal Unit Vectors (in Orbiter Reference System)

Components of the predicted and calculated surface normal unit vector are presented in Orbiter coordinates in Table 5-A. In addition, a precision estimate was generated by halving the difference between results obtained from the two cameras. Although not statistically based, this metric discriminates between the relative accuracies of each calculated vector component. This error is a function of camera resolution, field-of-view, panel orientation with respect to the camera optical axis, and the precision in defining image coordinates.

6. CORRELATION OF DOCKING EVENTS

Video of the Shuttle/Mir docking was analyzed to verify ring separation and the time of first contact. This analysis was performed at the request of engineers from the Structures and Dynamics Branch.

6.1 Motion Analysis at Soft Dock

Figure 6-A shows the camera A view of the Docking Module interface at the time of first contact. Two different types of video analysis were performed. The first procedure was to verify the time of first contact based on the motion of the washer seen on the centerline view. The second procedure was to determine the separation between the docking rings (identified by arrows) as a function of time. Both tasks were based on imagery acquired with the centerline camera.



Figure 6-A Centerline Video at First Contact

The crosshair alignment washer seen on the centerline video exhibits motion at the time of first contact with the Mir docking interface. Figure 6-A shows the centerline video view used in the analysis. Data was acquired over a 25-second interval. Edge-detection algorithms were used to track where the projected crosshair lines would intersect on each frame. Motion was measured using this intersection point for each frame with respect to the reference point (the fixed center of the alignment target). The distortions on the bottom of the video frame were attributed to problems with one of the onboard recorders.



Figure 6-B Docking Ring Interface at First Contact

An effort was also made to quantify the separation distance between the Orbiter and Mir docking rings through the time of initial contact. The arrows in Figure 6-B identify this distance on a camera A view. However, the actual analysis was performed on the centerline video data. The Mir standoff docking target was used as a scaling factor and the camera image plane location was estimated and used as the reference point to determine separation distance at the interface. In addition, the lateral motion of the standoff docking target was determined by measuring the distance between the center of the standoff docking target and the fixed center point of the image frame.

STS-76 Shuttle/Mir Motion Analysis at Docking

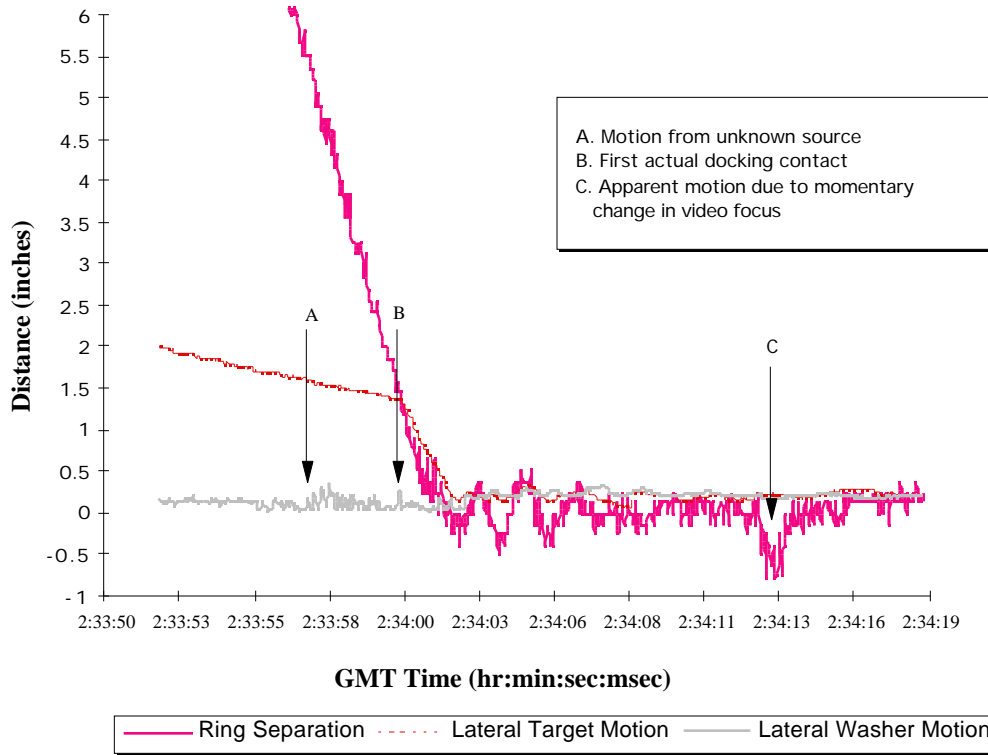


Figure 6-C Motion Analysis at Docking as a Function of Time

Figure 6-C shows the lateral motion of both the alignment washer and the standoff docking target, as well as the docking ring separation distance as a function of time. The separation distance was calculated based on an estimate of the camera image plane location and could account for the small negative numbers seen after first contact. Every video frame was used in the analysis for a period of approximately 26 seconds (or about 800 frames). Based on this data, the first contact between the Orbiter and Mir docking rings occurred at point 'B'. This information was forwarded to Structures and Dynamics engineers for additional assessment.

6.2 Sources of Error

Data in the vertical interval of the recorded video contains horizontal field-of-view information which is accurate to +/- 1 degree. This information is used in the calculation of the camera focal length and could contribute to errors in the analysis. Other sources of error could be attributed to an inaccurate estimate of the effective focal length of the camera (due to a lack of complete camera information) and the variability in focus at the time of docking. Although automated routines were used in the tracking of edges for this analysis, changes in the focus caused the apparent edge position to change creating false motion in the collected data (as seen in Figure 6-C).

7. MOTION ANALYSIS FROM FILM AND VIDEO

Information extracted from recorded video was used to calculate distances from the Shuttle to the Mir during approach and backaway. This procedure is being studied to determine its usefulness for future motion analysis of known objects in space where trajectory control data may not be available. Trajectory Control Systems (TCS) data available during the rendezvous served as ground truth for the analysis.

Video and photographic coverage of the Mir during approach and backaway were reviewed for this analysis. Measurements were made from the video to determine relative motion between the Shuttle and Mir during these times. Uncertainties about lenses used during the approach and backaway procedures precluded the use of still photography for this comparison.

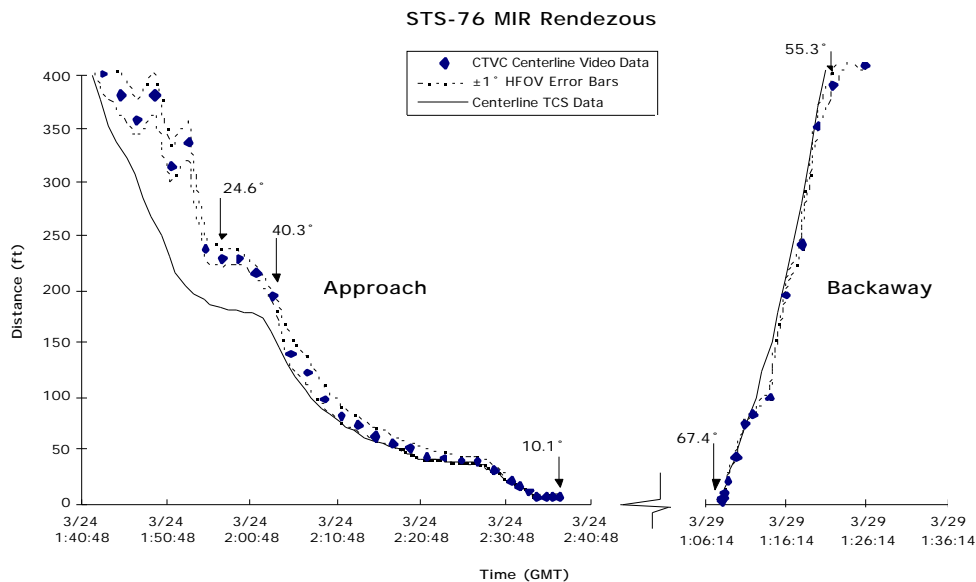


Figure 7-A Orbiter to Mir Distance Comparison using TCS and Video Data

Figure 7-A compares actual TCS data with CTVC video calculations. Horizontal-field-of-view (HFOV) information embedded in the vertical interval was used to calculate the separation distance between the Orbiter and the Mir. Each change in the HFOV is identified with an arrow in the graph above. These numbers have inherent errors of approximately $\pm 1^\circ$, and when propagated through photogrammetric equations, result in the error bars shown as dotted lines in the figure. The errors were on the order of $\pm 5^\circ$ when the Orbiter and Station docking interfaces were parallel. Other errors were induced during transition from one zoom setting to another. During approach, significant differences were observed beyond 150 feet between CTVC video calculations and TCS data. This was probably the result of two different error sources: poor lighting conditions, and wider fields of view which required the use of relatively small scaling targets. Note that the backaway video data (recorded in relatively good lighting conditions) correlates extremely well with the TCS data.

8. DEBRIS SEEN DURING DOCKING OPERATIONS

Small pieces of debris are seen on orbit during most missions. Several small pieces of debris were noted near the time of docking on STS-76. Three of these pieces of debris were tracked and characterized, and are considered representative of the particles seen around the time of docking. Velocity and size estimates were made using Docking Module features as scaling factors.

Prior to docking, nine small pieces of debris were seen in the vicinity of the payload bay, traveling toward the Station. In addition, one piece of debris appeared to originate from the Docking Module and travel toward the Orbiter. None of the visible debris was seen making contact with the Mir structure. However, the debris exited the camera field-of-view before any possible contact could be verified.

Figure 8-A Debris Near Payload Bay

Figure 8-A shows a camera A view of two pieces of debris that appeared to originate from the payload bay and travel toward the Mir. The velocity of these pieces were estimated to be approximately 2 inches per second. Neither piece appeared to impact the Station. These pieces were seen approximately two minutes before docking ring capture.



Figure 8-B Tumbling Debris from the Docking Module

Just prior to the docking ring capture, analysis was performed on a metallic-looking piece of debris that appeared to originate from a Cooperative Solar Array attach plate [identified by the box]. The debris appeared to be rotating and traveled towards the camera (located at the port forward corner of the Orbiter payload bay). The velocity of this single piece of debris was estimated at 5 inches per second. No damage was apparent on the available views.

9. IMAGERY EVALUATION

This section discusses overall quality of the film and video data obtained during DTO-1118. More detailed information about specific rolls of film and videotapes are included in Appendices B and C.

Imagery acquired of Mir surfaces during STS-76 consisted of the following:

- 20 hours of downlink and onboard video.
- 180 frames of 35 mm film.
- 1100 frames of 70 mm film.
- 28 Electronic Still Camera (ESC) images.

9.1 Video Review

The centerline camera provided the first views of the Mir approximately two hours before docking. The centerline camera views were downlinked through the final 250 feet of approach. During the dark phase of the orbit, only the blinking lights on the docking mechanism were visible on the available views. Varying focus and a zoomed-in field-of-view hampered analysis of the centerline video during the final docking procedure.

Much of the downlinked survey video was obtained via INCO ground control during three crew sleep periods of the docked phase. All four payload bay cameras were used in acquiring Mir survey imagery. This footage provided excellent coverage of the Orbiter-facing sides of the Spektr, Kvant-2, Base Block, Kristall and Kvant modules. In addition, systematic coverage of the newly installed Docking Module and the attached RSA and CSA carriers was obtained. Coverage of the Mir Environmental Effects Payload (MEEP) panels deployed on the Docking Module was obtained using three payload bay cameras. The Passive Optical Sample Assembly (POSA) panel surface was visible and mapped from PLB cameras B, C and D. The other three panels deployed were only visible from the aft cameras.

The centerline camera provided excellent views of the Mir docking interface area during the backaway sequence. Camera A was scheduled to be a "range ruler" for initial undocking and then tilted up to track any induced motion to the Base Block SP#2 array. However, by the time the array was properly centered within the field-of-view, the Mir was almost fifty feet away and no residual motion was seen. Some sun glare was initially visible on the camera A view, but this did not hamper analysis.

Fly-around coverage appeared to be limited to overview imagery. Payload bay cameras A, B and C, as well as the centerline camera, were used to acquire data during fly-around.

Several onboard videos were damaged due to problems with a recorder.

9.2 Still Photography Review

A few images of the Mir were acquired just after the attitude maneuver. Between 170 feet and 30 feet, the Mir was in darkness and no views of the docking mechanism were acquired using the Nikon (35 mm) camera. No views of the docking mechanism were

obtained during close approach (from 30 feet to 0 feet). As on STS-74, limited overhead window access time hampered data acquisition during this time period.

Overview coverage of the Orbiter-facing sides of Kvant, Spektr, Kvant-2, Kristall and Base Block modules was obtained using the Hasselblad camera. Some excellent images of the Base Block surface, Spektr SP#2 and Kvant-2 SP#2 solar arrays were captured with the 250mm lens on the Hasselblad. However, the surface of the Base Block was only mapped with the 40mm and 100mm lenses. This imagery provided limited detail of module surfaces.

No close-up images were obtained of the docking mechanism area during backaway.

Fly-around photography was limited to the Hasselblad camera with the 40mm lens. This imagery provided overview coverage of module surfaces that could only be seen during fly-around.

In summary, the limited photography acquired during approach and backaway made it difficult to evaluate the docking mechanism in detail. This mission generated some of the best imagery taken of the Spektr and Kvant-2 arrays. While good overview coverage of all modules was obtained, there was insufficient detail to evaluate possible orbital debris impacts on the Station.

10. CONCLUSIONS AND RECOMMENDATIONS

10.1 Summary

Imagery acquired with both the 70mm and 35mm still cameras provided adequate overview coverage of visible Mir surfaces throughout the mission. No still photographs of the docking mechanism area were acquired during the approach and backaway phases. Overview coverage of the Base Block, Kvant, Kvant-2 and Spektr module surfaces indicated no significant additional discoloration since the last rendezvous. The most significant anomalies from the STS-76 Mir survey were the peeling paint and discoloration seen on the Cooperative and Russian Solar Array carriers attached to the Docking Module. New areas of peeling paint were also detected on the Spektr radiator. In addition, several small discolored areas were identified on the detailed coverage of Spektr arrays. No Mir solar array motion was detected from the available video during the rendezvous. Use of INCO-controlled payload bay cameras to perform video surveys during sleep periods provided good coverage of areas of Mir not visible from Shuttle windows. In addition, a survey of the newly installed Mir Environmental Effects Payload (MEEP) panels was performed to determine the experiment's initial condition.

The combined imagery gathered on the STS-63, STS-71, STS-74, and STS-76 missions provide significant information from which a subjective assessment can be made about effects of the space environment on an orbiting platform.

10.2 Conclusions

Based on the summary of major points made above, the following conclusions can be made:

Crew time constraints and limited window accessibility severely hampered data acquisition during approach and backaway.

Use of shorter focal length lenses during the docked phase did not provide adequate detailed coverage of module surfaces.

Use of shorter focal length lenses during the fly-around limited coverage of Mir surfaces not visible during the docked phase.

Equipment and time constraints precluded video acquisition of solar arrays during certain phases of the rendezvous when array motion may have otherwise been visible. In addition, conflicts with other DTOs have led to limited coverage of possible array motion events.

INCO-controlled video surveys during crew sleep periods provided the best available coverage of the MEEP panels on the Docking Module.

Centerline video acquired during approach and backaway provided the best views of the docking mechanism area (to verify the condition of latches and targets). Still photography was not acquired during the same time period.

10.3 Recommendations

Based on the summary above, crew comments during training, and evaluation of the STS-76 imagery, the following recommendations can be made for upcoming rendezvous missions:

Centerline video camera views of the docking area should be the primary source for determining the condition of the target, docking ring and latches, since the crew has limited accessibility to windows for photography during approach and backaway.

The Nikon should be used as the primary camera during approach, backaway, and fly-around instead of the Hasselblad. This recommendation is based on crew comments that bracketing with the Nikon would be easier during these events and also because it would allow use of the 300mm lens during the fly-around.

The Hasselblad with the 250mm lens should be used as the primary camera/lens combination to identify possible orbital debris impacts on module surfaces. The wider format film provides more contextual information and the longer lens provides more detail.

Generate an updated mission-specific target priority list for the crew at the last training session. Configuration modifications and varying image acquisition requirements justify the need for an updated list.

Continue to use INCO-controlled payload bay video cameras to perform Mir surveys during crew sleep periods. This has been the most effective way to obtain survey video coverage and also allows real-time decisions to be made on target acquisition.

Re-evaluate the priority of acquiring unanticipated solar array motion from payload bay video cameras during approach and backaway.

Continue to emphasize the need for bracketing exposures when acquiring imagery.

Request the crew to be aware of lighting conditions that highlight surface features. Lighting angles oblique to Mir surfaces convey textural information that would otherwise remain hidden.

Fill at least one video camera field-of-view with the Mir during fly-around. Unanticipated array motion would be easier to detect with this configuration.

11. REFERENCES

Bluth, B. J., D. Fielder, Soviet Space Stations as Analogs, Vol. II, 3rd Edition, September 1993.

Gaskill, J. D., Linear Systems, Fourier Transforms, and Optics, John Wiley & Sons, New York, New York, 1978.

Lillesand, T. M., R. W. Kiefer, Remote Sensing and Image Interpretation, John Wiley & Sons, New York, New York, 1979.

NASA/RSC-E Joint Report, Mir Photo/TV Survey (DTO-1118): STS-63, JSC-27246, August 28, 1995.

NASA/RSC-E Joint Report, Mir Photo/TV Survey (DTO-1118): STS-71, JSC-27355 January 16, 1996.

Mir Photo/TV Survey (DTO-1118): STS-74 Mission Report, JSC-27383, February 29, 1996.

Mission Operations Directorate, Space Flight Training Division, Systems Training Branch, A Russian Space Station: The Mir Complex, National Aeronautics and Space Administration, Lyndon B. Johnson Space Center, Houston, Texas, February 1994.

NASA Drawing Package, STS-76 Shuttle Mir Docking Mission, WG-3/RSC-E/NASA/003/3402-3, December 15, 1995.

Portree, David S. F., Information Services Division, Mir Hardware Heritage, JSC 26770, Lyndon B. Johnson Space Center, Houston, Texas, October 1994.